Characterization of *Mollivirus kamchatka*, the first modern representative of the proposed *Molliviridae* family of giant viruses.

Running title: characterization of the first modern mollivirus

Eugene Christo-Foroux[#a], Jean-Marie Alempic[a], Audrey Lartigue[a], Sebastien Santini[a], Karine Labadie[b], Matthieu Legendre[a] , Chantal Abergel[a] , Jean-Michel Claverie[#a]

a Aix Marseille Univ., CNRS, IGS, Information Génomique & Structurale (UMR7256), Institut de Microbiologie de la Méditerranée (FR 3489), Marseille, France

b Genoscope, Institut François Jacob, CEA, Université Paris-Saclay, Évry, France

Correspondance to: Eugene.christo-foroux@igs.cnrs-mrs.fr, jean-michel.claverie@univ-amu.fr

Keywords: Paleovirology; Kamchatka; Comparative Genomics; Nucleo-cytoplasmic Large DNA viruses; Genome Structure.

Abstract

Microbes trapped in permanently frozen paleosoils (permafrost) are the focus of increasing researches in the context of global warming. Our previous investigations led to the discovery and reactivation of two Acanthamoeba-infecting giant viruses, *Mollivirus sibericum* and *Pithovirus sibericum* from a 30,000-year old permafrost layer. While several modern pithovirus strains have since been isolated, no contemporary mollivirus relative was found. We now describe *Mollivirus kamchatka*, a close relative to *M. sibericum*, isolated from surface soil sampled on the bank of the Kronotsky river in Kamchatka. This discovery confirms that molliviruses have not gone extinct and are at least present in a distant subarctic continental location. This modern isolate exhibits a nucleo-cytoplasmic replication cycle identical to that of *M. sibericum*. Its spherical particle (0.6-µm in diameter) encloses a 648-kb GC-rich double stranded DNA genome coding for 480 proteins of which 61 % are unique to these two molliviruses. The 461 homologous proteins are highly conserved (92 % identical residues in average) despite the presumed stasis of *M. sibericum* for the last 30,000 years. Selection pressure analyses show that most of these proteins contribute to the virus fitness. The comparison of these first two molliviruses clarify their evolutionary relationship with the pandoraviruses, supporting their provisional classification in a distinct family, the *Molliviridae*, pending the eventual discovery of intermediary missing links better demonstrating their common ancestry.

43

44 **Importance**

45 Virology has long been viewed through the prism of human, cattle or plant diseases leading to a
46 largely incomplete picture of the viral world. The serendipitous discovery of the first giant virus
47 visible under light microscopy (i.e., >0.3µm in diameter), mimivirus, opened a new era of
48 environmental virology, now incorporating protozoan-infecting viruses. Planet-wide isolation
49 studies and metagenomes analyses have shown the presence of giant viruses in most terrestrial
50 and aquatic environments including upper Pleistocene frozen soils. Those systematic surveys have
51 led authors to propose several new distinct families, including the *Mimiviridae*, *Marseilleviridae*,
52 *Faustoviridae*, *Pandoraviridae*, and *Pithoviridae*. We now propose to introduce one additional
53 family, the *Molliviridae*, following the description of *M. kamchatka*, the first modern relative of *M.*
54 *sibericum*, previously isolated from 30,000-year old arctic permafrost.

55

56

57 **Introduction**

58 Studies started about 30 years ago, have provided multiple evidence that soils frozen since the late
59 Pleistocene and predominantly located in arctic and subarctic Siberia, do contain a wide diversity
60 of microbes that can be revived upon thawing (1-3) after tens of thousands of years. These studies
61 culminated by the regeneration of a plant from 30,000 year-old fruit tissue (4). Inspired by those
62 studies, we then isolated from a similar sample two different Acanthamoeba-infecting large DNA
63 viruses, named *Pithovirus sibericum* and *Mollivirus sibericum*, demonstrating the ability for these
64 viruses, and maybe many others, to remain infectious after similarly long periods of stasis in
65 permafrost (5-6). Several modern relatives to the prototype Pithovirus have since been isolated
66 and characterized, leading to the emergence of the new proposed *Pithoviridae* family (7-10). In
67 contrast, and despite the increasing sampling efforts deployed by several laboratories, no other
68 relative of *M. sibericum* was found. Without additional isolates, its classification as a prototype of a
69 new family, or as a distant relative of the pandoraviruses (with which it shared several
70 morphological features and 16% of its gene content) (6) remained an open question. Here we
71 report the discovery and detailed characterization of the first modern *M. sibericum* relative,
72 named *Mollivirus kamchatka*, after the location of the Kronotsky river bank where it was retrieved.
73 The comparative analysis of these first two molliviruses highlights their evolutionary processes and
74 suggests their provisional classification into their own family, the *Molliviridae*, distinct from the
75 *Pandoraviridae*, pending the eventual discovery of intermediary missing links clearly establishing
76 their common ancestry.

77

78

79 **Results**

80 **Virus isolation**

81 The original sample consisted of about 50 ml of vegetation-free superficial soil scooped (in sterile
82 tubes) from the bank of the Kronotsky river (coordinates: N 54°32'59'' E 160°34'55'') on july 6th,
83 2017. Before being stored at 4°C, the sample was transported in a backpack for a week at ambient
84 temperature (5° C up to 24° C). This area corresponds to a continental subarctic climate: very cold
85 winters, and short, cool to mild summers, low humidity and little precipitation. Back in the
86 laboratory, few grams of the sample were used in the Acanthamoeba co-cultivation procedure
87 previously described (6). After a succession of passages and enrichment on *Acanthamoeba*
88 *castellanii* cultures, viral particles were produced in sufficient quantity to be recovered and
89 purified.

90 **Virion morphology and ultrastructure**

91 As for *M. sibericum*, light microscopy of infected cultures showed the multiplication of particles.
92 Using transmission electron microscopy (TEM), these particles - undistinguishable from that of *M.*
93 *sibericum* - appear approximately spherical, 600 nm in diameter, lined by an internal lipid
94 membrane and enclosed in a 20 nm-thick electron-dense thick tegument covered with a mesh of
95 fibers (Fig. 1).

96 **Analysis of the replication cycle**

97 The replication cycle in *A. castellanii* cells was monitored using TEM and light microscopy of DAPI-
98 stained infected cultures as previously described (6). The suite of events previously described for
99 host cells infected by *M. sibericum*, was similarly observed upon *M. kamchatka* replication (6, 11).
100 After entering the amoeba cell through phagocytosis, *M. Kamchatka* virions are found gathered in
101 large vacuoles individually or in groups of 2-6 particles. Multiple nuclear events occur during the
102 infection starting with the drift of the host cell nucleolus to the periphery of the nucleus 4-5h post
103 infection (p.i.). 7h p.i., the nucleus appears filled with numerous fibrils that may correspond to viral

104 genomes tightly packed in DNA-protein complexes (Fig. 2A). About 30% of the nuclei observed at
105 that time exhibit a ruptured nuclear membrane (Fig. 2B). Besides those internal nuclear events, we
106 observed a loss of vacuolization within the host cell from 4h p.i. to the end of the cycle, in average
107 9h p.i.. Large viral factories are formed in the cytoplasm at the periphery of the disorganized
108 nucleus (Fig. 2). These viral factories displays the same characteristics as those formed during *M.*
109 *sibericum* infections, involving an active recycling of membrane fragments (11).

110 **Comparative genomics**

111 DNA prepared from purified *M. kamchatka* particles was sequenced using both Illumina and
112 Oxford Nanopore platforms. *M. kamchatka* genome, a linear double stranded DNA molecule
113 (dsDNA), was readily assembled as a unique sequence of 648,864 bp. The read coverage was
114 uniform throughout the entire genome except for a 10 kb terminal segment presumably repeated
115 at both ends and exhibiting twice the average value. The *M. kamchatka* genome is thus
116 topologically identical to that of a *M. sibericum*, slightly larger in size (when including both terminal
117 repeats), and with the same global nucleotide composition (G+C= 60%). This similarity was
118 confirmed by the detailed comparison of their genome sequences exhibiting a global collinearity
119 solely interrupted by a few insertions and deletions.

120 Prior to the comparison of their gene contents, *M. sibericum* and *M. kamchatka* were both
121 annotated using the same stringent procedure that we previously developed to correct for gene
122 overpredictions suspected to occur in G+C rich sequences such as those of pandoraviruses (12-14).
123 A total of 495 and 480 genes were predicted for *M. sibericum* and *M. kamchatka*, with the
124 encoded proteins ranging from 51 to 2171 residues and from 57 to 2176 residues, respectively.
125 *M. kamchatka* predicted protein sequences were used in similarity search against the non-
126 redundant protein sequence database (15) and the re-annotated *M. sibericum* predicted
127 proteome. Out of the 480 proteins predicted to be encoded by *M. kamchatka* 463 had their closest
128 homologs in *M. sibericum*, with 92% identical residues in average. After clustering the paralogs,

129 these proteins corresponded to 434 distinct genes clusters delineating a first estimate of the
130 mollivirus core gene set. Four hundred and eleven of these clusters contained a single copy
131 (singletons) gene for each strain. Remarkably, 290 of the 480 (60.4 %) *M. kamchatka*-encoded
132 proteins did not exhibit a detectable homolog among cellular organisms or previously sequenced
133 viruses (excluding *M. sibericum*). Those will be referred to as "ORFans". Among the 190 proteins
134 exhibiting significant ($E<10^{-5}$) matches in addition to their *M. sibericum* counterparts, 78 (16% of
135 the total gene content) were most similar to Pandoravirus predicted proteins, 18 (3.7%) to proteins
136 of other virus families, 51 (10.6%) to *A. castellanii* proteins, 24 (5%) to proteins of other
137 eukaryotes, 17 (3.5%) to bacterial proteins and 2 (0.4%) to proteins of *Archaea* (Fig. 3).
138 The interpretation of these statistics are ambiguous as, on one hand, the large proportion of
139 "ORFans" (>60%) is characteristic of what is usually found for the prototypes of novel giant virus
140 families (7). On the other hand, the closest viral homologs are not scattered in diverse previously
141 defined virus families, but mostly belongs to the Pandoraviridae (78/96=81%) (Fig. 3). The two
142 molliviruses thus constitute a new group of viruses with their own specificity but with a
143 phylogenetic affinity with the pandoraviruses, as previously noticed (7). The proportion of *M.*
144 *kamchatka* proteins with best matching counterparts in Acanthamoeba confirms the high gene
145 exchange propensity with the host, already noticed for *M. sibericum* (6).

146 **Recent evolutionary events since the *M. sibericum*/*M. kamchatka* divergence**

147 We investigated the evolutionary events specific of each of the molliviruses by focusing on proteins
148 lacking reciprocal best matches between the two strains. We found 63 such cases of which 10
149 corresponded to unilateral strain-specific duplications of genes, and 53 were unique to a given
150 strain. These unique genes (Table 1 & 2) result from gains or losses in either of mollivirus strains
151 (20 in *M. Kamchatka*, 33 in *M. sibericum*). The likely origins of these strain-specific genes
152 (horizontal acquisition, *de novo* creation (13, 14), or differential loss) are listed in Table 1 and Table
153 2.

154 Six *M. kamchatka* proteins, absent from *M. sibericum*, have homologs in pandoraviruses
155 suggesting common gene ancestors (and loss in *M. sibericum*) or horizontal acquisitions. According
156 to its embedded position within the pandoravirus phylogenetic tree, only one anonymous protein
157 (mk_165) could be interpreted as a probable horizontal transfer from pandoraviruses (Fig. 4A).
158 Another candidate, mk_92, shares 75% of identical residues with a pandoravirus DNA
159 methyltransferase (pqer_cds_559). However the very long branch associated to the P. dulcis
160 homolog (eventually due to a non-orthologous replacement) raises some doubt as for the origin of
161 the *M. kamchatka* gene (Fig. 4B).
162 Two *M. kamchatka*-specific proteins, encoded by adjacent genes (mk_466, mk_467), have
163 homologs in Acanthamoeba, suggesting potential host-virus exchanges. Phylogenetic
164 reconstruction did not suggest a direction for the transfer of mk_466. However, since the unique
165 homolog of mk_467 is found in Acanthamoeba (and not in other eukaryotes), the corresponding
166 gene probably originated from a close relative of *M. kamchatka* and was recently transferred to its
167 host.
168 Three proteins unique to *M. sibericum* have homologs in pandoraviruses (Table 2), suggesting
169 common gene ancestors (and loss in *M. kamchatka*) or horizontal acquisitions. One protein
170 (ms_14) has a unique homolog in Acanthamoeba, suggesting a virus to host exchange. The
171 homolog of ms_312 in *Cavenderia fasciculata* (16) might be the testimony of past interactions
172 between molliviruses and deeply rooted ancestor of the Amoebozoa clade.
173 The above analyses of the genes unique to each mollivirus indicate that if horizontal transfer
174 may contribute to their presence, it is not the predominant mechanisms for their acquisition. We
175 then further investigated the 12 genes unique to *M. kamchatka* and 26 genes unique to *M.*
176 *sibericum* (i.e. “strain ORFans” w/o homolog in the databases) by computing three independent
177 sequence properties (Fig. 5): the codon adaptation usage index (CAI), the G+C composition, and
178 the ORF length.

179 With an average CAI value of 0.26, the strain-specific ORFans appear significantly different
180 from the rest of the mollivirus genes (mean = 0.40, Wilcoxon test $p < 2\ 10^{-7}$). These genes also
181 exhibit a significantly lower G+C content (56% for *M. kamchatka* and 57% for *M. sibericum*) than
182 the rest of the genes (60.5% for both viruses), also closer to the value computed for intergenic
183 regions (54% in average for both viruses). Moreover, the strain-specific ORFans are smaller in
184 average compared to the rest of the genes (115bp/378bp for *M. kamchatka* and 122bp/369bp for
185 *M. sibericum*). Altogether, those results suggest that *de novo* gene creation might occur in the
186 intergenic regions of molliviruses as already postulated for pandoraviruses (13, 14).

187 **New predicted protein functions in *M. kamchatka***

188 Sixty four of the *M. kamchatka* predicted proteins exhibit sequence motifs associated to known
189 functions. Fifty nine of them are orthologous to previously annotated genes in *M. sibericum* (6).
190 This common subset confirms the limited complement of DNA processing and repair enzymes
191 found in molliviruses: mainly a DNA polymerase: mk_287, a primase: mk_236, and 3 helicases:
192 mk_291, mk_293, mk_351. *M. kamchatka* confirms the absence of key deoxynucleotide synthesis
193 pathways (such as thymidylate synthase, thymidine kinase and thymidylate kinase), and of a
194 ribonucleoside-diphosphate reductase (present in pandoraviruses). The five *M. kamchatka* specific
195 proteins (Table 1) associated to functional motifs or domain signature correspond to:
196 - two proteins (mk_93 and mk_104) containing a type of zinc finger (Ring domain) mediating
197 protein interactions,
198 - one protein (mk_469) with similarity to the (BI)-1 like family of small transmembrane proteins,
199 - one predicted LexA-related signal peptidase (mk_166),
200 - one DNA methyltransferase (mk_92).

201 **Evaluation of the selection pressure exerted on mollivirus genes**

202 The availability of two distinct strains of mollivirus allows the first estimation of the selection
203 pressure exerted on their shared genes during their evolution. This was done by computing the

204 ratio ω=dN/dS of the rate of non-synonymous mutations (dN) over the rate of synonymous
205 mutations (dS) for pairs of orthologous genes. ω values much lesser than one are associated to
206 genes the mutation of which have the strongest negative impact on the virus fitness. The high
207 sequence similarity of proteins shared by *M. sibericum* and *M. kamchatka* allowed the generation
208 of flawless pairwise alignments and the computation of highly reliable ω values for most (*i.e.*
209 397/411) of their orthologous singletons.

210 Fourteen singleton pairs were not taken into account in the selection pressure analysis
211 because of their either identical or quasi-identical sequences (11 of them), or unreliable pairwise
212 alignments (3 of them). For the 397 gene pairs retained in the analysis, the mean ω value was 0.24
213 ± 0.14 (Fig. 6). This result corresponds to a strong negative selection pressure indicating that most
214 of the encoded proteins greatly contribute to the molliviruses' fitness. Together with the high level
215 of pairwise similarity (92%) of their proteins, this also indicates that *M. kamchatka* evolved very
216 little during the last 30,000 years and that the *M. sibericum* genome was not prominently damaged
217 during its cryostasis in permafrost.

218 The analysis restricted to the 244 pairs of ORFan-coding genes resulted in a very similar ω
219 value of 0.29± 0.15 (Fig. 6). This indicates that although homologs of these proteins are only found
220 in molliviruses, they have the same impact on the virus fitness than more ubiquitous proteins. This
221 confirms that they do encode actual proteins, albeit with unknown functions. In contrast, four
222 orthologous pairs (ms_160/mk_141; ms_280/mk_262; ms_171/mk_151; ms_430/mk_411;
223 ms_60/mk_48) exhibit ω value larger than one. Those ORFans either are under positive selection
224 for maintaining their functions, or newly created gene products undergoing refinement or
225 pseudogenization.

226 We further examined the selection pressure of proteins-coding genes with homologs in
227 pandoraviruses. We used their 10 sequenced genomes to generate the corresponding gene
228 clusters (Fig. 7). The 90 clusters shared by both virus groups included 64 singletons (single copy

229 gene present in all viruses), among which 55 were suitable for dN/dS computations. The mean ω
230 value (0.17 ± 0.1) was very low, indicating that these genes, forming a "super core" gene set
231 common to the molliviruses and pandoraviruses, are under an even stronger negative selection
232 pressure than those constituting the provisional (most likely overestimated) mollivirus core gene
233 set .

234 **Genomic inhomogeneity**

235 The original genome analysis of Lausannevirus (a member of the Marseilleviridae family) (17)
236 revealed an unexpected non-uniform distribution of genes according to their annotation.
237 "Hypothetical" genes (i.e. mostly ORFans) were segregated from "annotated" (i.e. mostly non-
238 ORFans) in two different halves of the genome. In a more recent work, we noticed a similar bias in
239 the distribution of Pandoravirus core genes (13). The availability of a second mollivirus isolate gave
240 us the opportunity to investigate this puzzling feature for yet another group of Acantamoeba-
241 infecting virus. In Fig. 8, we plotted the distribution of three types of genes: 1- those with
242 homologs in *A. castellanii* (n= 55 for *M. sibericum* and n= 51 for *M. kamchatka*), 2- those belonging
243 to the super core set shared by both molliviruses and pandoraviruses (n=64), 3- those unique to
244 either mollivirus strains (n=26 for *M. sibericum*, n=12 for *M. kamchatka*). These plots reveal a
245 strong bias in the distribution of the super core vs. ORFan genes (Fig. 8). The first half of the *M.*
246 *sibericum* genome exhibits 90% of its ORFans while the second half contains most of the members
247 of the super core gene set. In contrast, genes eventually exchanged with the host display a more
248 uniform distribution. The lack of an apparent segregation in the distribution of ORFans in the *M.*
249 *kamchatka* genome might be due to their underprediction as no transcriptome information is
250 available for this strain. Fig. 9 shows that there is also a strong bias in the distribution of single-
251 copy genes *vs.* those with paralogs in either *M. sibericum* and/or *M. kamchatka*. Altogether, these
252 analyses suggest that the two genome halves follow different evolutionary scenario, the first half

253 concentrating the genomic plasticity (*de novo* gene creation, gene duplication), the other half
254 concentrating the most conserved, eventually essential, gene content.
255
256 **Discussion**
257 Following the discovery of their first representatives, each families of giant (e.g. Mimiviridae,
258 Pithoviridae, Pandoraviridae) and large (e.g. Marseilleviridae) viruses infecting acanthamoeba have
259 expanded steadily, suggesting they were relatively abundant and present in a large variety of
260 environments. One noticeable exception has been the molliviruses, the prototype of which
261 remained unique after its isolation from 30,000-year old permafrost. The absence of *M. sibericum*
262 relatives from the large number of samples processed by others and us since 2014, raised the
263 possibility that they might have gone extinct, or might be restricted to the Siberian arctic. Our
264 isolation of a second representative of the proposed Molliviridae family, *M. kamtchatka*, at a
265 location more than 1,500 km from the first isolate and enjoying a milder climate, is now refuting
266 these hypotheses. Yet, the planet-wide ubiquity of these viruses remains to be established, in
267 contrast to other acanthamoeba-infecting giant viruses (7). Even when present, mollivirus-like
268 viruses appear to be in very low abundance, as judged from the very small fraction of
269 metagenomics reads they represent in total sample DNA for *M. kamchatka* (about 0.02 part per
270 million) as well as for *M. sibericum* (about one part per million)(6). Another possibility would be
271 that the actual environmental host is not an acanthamoeba, the model host used in our laboratory.
272 However, evidences of specific gene exchanges with acanthamoeba (including a highly conserved
273 homolog major capsid protein) (6, 18, 19) make this explanation unlikely. We conclude that
274 members of the proposed Molliviridae family are simply less abundant than other acanthamoeba-
275 infecting viruses, a conclusion further supported by the paucity of Mollivirus-related sequences in
276 the publicly available metagenomics data (data not shown).

277 As always the case, the characterization of a second representative of a new virus
278 representative opened new opportunities of analysis. Unfortunately, the closeness of *M.*
279 *kamchatka* with *M. sibericum* limited the amount of information that could be drawn from their
280 comparison. For instance, the number of genes shared by the two isolates is probably a large
281 overestimate of the "core" gene set characterizing the whole family. On the other hand, the
282 closeness of the two isolates allowed an accurate determination of the selection pressure
283 (ω=dN/dS) exerted on many genes, showing that most of them, including mollivirus ORFans,
284 encode actual proteins the sequence of which are under strong negative selection and thus
285 contribute to the virus fitness. Given the partial phylogenetic affinity (i.e. 90 shared gene clusters)
286 of the mollivirus with the pandoraviruses, we also assessed the selection pressure exerted on 55 of
287 these "super core" genes, and found them under even stronger negative selection (Fig. 7). This
288 suggests that this super core gene set might have been present in a common ancestor to both
289 proposed families.
290 If we postulate that *M. sibericum* underwent into a complete stasis when it became frozen in
291 permafrost while *M. kamchatka* remained in contact with living acanthamoeba, we could consider
292 the two viral genomes to be separated by at least 30,000 years of evolution (eventually more if
293 they are not in a direct ancestry relationship)(20). The high percentage of identical residues (92%)
294 in their proteins corresponds to a low substitution rate of 1.7 10^{-6} amino acid change/position
295 /year. This is an overestimate since the two viruses probably started to diverge from each other
296 longer than 30,000-year ago. This value is nevertheless comparable with estimates computed for
297 poxviruses (21) given the uncertainty on the number of replicative cycles occurring per year. The
298 high level of sequence similarity of *M. kamchatka* with *M. sibericum* also indicates that the later
299 did not suffer much DNA damage during its frozen stasis, even in absence of detectable virus-
300 encoded DNA repair functions.

301 Horizontal gene transfers with the host were suggested by the fact that 51 proteins shared by
302 the two mollivirus strains exhibited a second best match in acanthamoeba. Because no homolog is
303 detected in other eukaryotes for most of them, these transfers probably occurred in the mollivirus-
304 to-host direction. The clearest case is that of a major capsid protein homolog (mk_314, ml_347)
305 sharing 64% identical residues with a predicted acanthamoeba protein (locus: XP_004333827).
306 Two other genes encoding proteins that have also homologs in molliviruses flank the
307 corresponding host gene. However, the corresponding viral genes are not collinear in *M. sibericum*
308 or *M. kamchatka* and were probably transferred from a different, yet unknown mollivirus strain.
309 The presence of a 100% conserved major capsid protein homolog in the genome of *M. kamchatka*
310 and *M. sibericum* is itself puzzling. Such protein (with a double-jelly roll fold) is central to the
311 structure of icosahedral particles (22). Consistent with its detection in *M. sibericum* virions (6), its
312 conservation in *M. kamchatka*, suggests that it still plays a role in the formation of the spherical
313 mollivirus particles, while it has no homolog in the pandoraviruses. Inspired by previous
314 observations made on the unrelated Lausannevirus genome (17), we unveiled a marked
315 asymmetry in the distribution of different types of protein-coding genes in the Mollivirus genomes.
316 As shown in Fig. 8 the left half of the genome concentrates most of the genes coding for strain-
317 specific ORFans while the right half concentrates most of super core genes shared with
318 pandoraviruses. This asymmetry is even stronger for the multiple copy genes while single-copy
319 genes are uniformly distributed along the genome (Fig. 9). The molliviruses thus appear to confine
320 their genomic "creativity" (*de novo* creation and gene duplication) in one-half of their genome,
321 leaving the other half more stable. An asymmetry in the distribution of the core genes was
322 previously noticed in the pandoravirus genomes (13). Such features might be linked to the
323 mechanism of replication that is probably similar for the two virus families. Further studies are
324 needed to investigate this process. The asymmetrical genomic distribution of pandoravirus core
325 genes and mollivirus super core genes might be a testimony of their past common ancestry.

326 Despite their differences in morphology, as well as in virion and genome sizes, the comparative
327 analysis of the prototype *M. sibericum* and of the new isolate *M. kamchatka* confirms their
328 phylogenetic affinity with the Pandoraviruses (Fig. 3, Fig. 10). However, it remains unclear whether
329 this is due to a truly ancestral relationship between them, or if it is only the consequence of
330 numerous past gene exchanges favored by the use of the same cellular host. From the perspective
331 of the sole DNA polymerase sequence, the two known molliviruses do cluster with the
332 pandoraviruses, albeit at a larger evolutionary distance than usually observed between members
333 of the same virus family (Fig. 10). In absence of an objective threshold, and pending the
334 characterization of eventual "missing links", we thus propose to classify *M. sibericum* and *M.*
335 *kamchatka* as members of the proposed Molliviridae family, distinct from the Pandoraviridae.
336

337 **Materials and Methods**

338 **Virus isolation**

339 We isolated *M. kamchatka* from muddy grit collected near Kronotski Lake, Kamchatka (Russian
340 Federation N :54 32 59, E :160 34 55). The sample was stored for twenty days in pure rice medium
341 (23) at room temperature. An aliquot of the pelleted sample triggered an infected phenotype on a
342 culture of *Acanthamoeba castellanii Neff* (ATCC30010TM) cells adapted to 2,5µg/mL of
343 Amphotericin B (Fungizone), Ampicillin (100µg/ml), Chloramphrenicol (30µg/ml) and Kanamycin
344 (25µg/ml) in protease-peptone–yeast-extract–glucose (PPYG) medium after two days of incubation
345 at 32°C. A final volume of 6 mL of supernatant from two T25 flasks exhibiting infectious
346 phenotypes was centrifuged for 1 hour at 16,000xg at room temperature. Two T75 flasks were
347 seeded with 60,000 cells/cm² and infected with the resuspended viral pellet. Infected cells were
348 cultured in the same conditions as described below. We confirmed the presence of viral particles
349 by light microscopy.

350 **Validation of the presence of *M. kamchatka* in the original sample**

351 To confirm the origin of the *M. kamchatka* isolate from the soil of the Kronotsky river bank,
352 DNA was extracted from the sample and sequenced on an Illumina platform, leading to
353 340,320,265 pair-ended reads (mean length 150bp). These metagenomics reads were then
354 mapped onto the genome sequence of *M. kamchatka*. Seven matching (100 % Identity) pair-ended
355 reads (hence 14 distinct reads) were detected, indicating the presence of virus particles in the
356 original sample, although at very low concentration. However, the very low probability of such
357 matches by chance ($p<10^{-63}$) together with the scattered distribution of these matches along the
358 viral genome, further demonstrate the presence of *M. kamchatka* in the original sample.
359

360 **Virus Cloning**

361 Fresh *A. castellanii* cells were seeded on a 12-well culture plate at a final concentration of
362 70,000cells/cm². Cell adherence was controlled under light microscopy after 45 minute and viral
363 particles were added to at a multiplicity of infection (MOI) around 50. After 1 h, the well was
364 washed 15 times with 3 mL of PPYG to remove any viral particle in suspension. Cells were then
365 recovered by gently scrapping the well, and a serial dilution was performed in the next three wells
366 by mixing 200µL of the previous well with 500µL of fresh medium. Drops of 0.5µL of the last
367 dilution were recovered and observed by light microscopy to confirm the presence of a unique *A.*
368 *castellanii* cell. The 0.5µL droplets were then distributed in each well of three 24-well culture plate.
369 Thousand uninfected *A. castellanii* cells in 500µL of PPYG were added to the wells seeded with a
370 single cell and incubated at 32°C until witnessing the evidence of a viral production from the
371 unique clone. The corresponding viral clones were recovered and amplified prior purification, DNA
372 extraction and cell cycle characterization by electron microscopy.

373 **Virus mass production and purification**

374 A total number of 40 T75 flasks were seeded with fresh *A. castellanii* cells at a final
375 concentration of 60,000 cells/cm². We controlled cell adherence using light microscopy after 45

376 minute and flasks were infected with a single clone of *M. kamchatka* at MOI=1. After 48h hours of
377 incubation at 32°C, we recovered cells exhibiting infectious phenotypes by gently scrapping the
378 flasks. We centrifuged for 10 min at 500×g to remove any cellular debris and viruses were pelleted
379 by a 1-hour centrifugation at 6,800xg. The viral pellet was then layered on a discontinuous cesium
380 chloride gradient (1,2g/cm²/ 1,3g/cm²/ 1,4g/cm²/ 1,5g/cm²) and centrifuged for 20h at 103,000xg.
381 The viral fraction produced a white disk, which was recovered and washed twice in PBS and stored
382 at 4 °C or −80 °C with 7,5% DMSO.
383
384 **Infectious cycle observations using TEM**
385 Twelve T25 flasks were seeded with a final concentration of 80,000 cells/cm² in PPYG medium
386 containing antibiotics. In order to get a synchronous infectious cycle eleven flasks were infected by
387 freshly produced *M. kamchatka* at substantial MOI=40. The *A. castellanii* infected flasks were fixed
388 by adding an equal volume of PBS buffer with 5 % glutaraldehyde at different time points after the
389 infection : 1h pi, 2h pi, 3h pi, 4h pi, 5h pi, 6h pi, 7h pi, 8h pi, 9h pi, 10h pi and 25h pi. After 45min of
390 fixation at room temperature, cells were scrapped and pelleted for 5min at 500xg. Then cells were
391 resuspended in 1ml of PBS buffer with 2,5 % glutaraldehyde and stored at 4°C. Each sample was
392 coated in 1mm³ of 2 % low melting agarose and embedded in Epon-812 resin. Optimized osmium-
393 thiocarbohydrazide-osmium (OTO) protocol was used for staining the samples: 1h fixation in PBS
394 with 2 % osmium tetroxide and 1.5 % potassium ferrocyanide, 20 min in water with 1 %
395 thiocarbohydrazide, 30min in water with 2 % osmium tetroxide, overnight incubation in water with
396 1 % uranyl acetate and finally 30min in lead aspartate. Dehydration was made using an increasing
397 concentration of ethanol (50 %, 75 %, 85 %, 95 %, 100 %) and cold dry acetone. Samples were
398 progressively impregnated with an increasing mix of acetone and Epon-812 resin mixed with DDSA
399 0,34v/v and NMA 0,68v/v (33 %, 50 %, 75 % and 100%). Final molding was made using a hard
400 Epon-812 mix with DDSA 0,34v/v NMA 0,68v/v and 0,031v/v of DMP30 accelerator and hardened

401 in the oven at 60°C for 5 days. Ultrathin sections (90nm thick) were observed using a FEI Tecnai G2
402 operating at 200kV.

403 **DNA Extraction**

404 *M. kamchatka* genomic DNA was extracted from approximately 5 x 10^9 purified virus particles
405 using Purelink Genomic extraction mini kit according to the manufacturer's recommendation. Lysis
406 was performed with in a buffer provided with the kit and extra DTT at a final concentration of
407 1mM.

408 **Genome sequencing and assembly**

409 *M. kamchatka* genome was assembled using Spades (24) with a stringent K-mer parameter
410 using both various iteration steps (k = 21,41,61,81,99,127), the "-careful" option to minimize
411 number of mismatches in the final contigs, and the "-nanopore" option to use long reads.

412 **Annotation of *Mollivirus sibericum* and *Mollivirus kamchatka***

413 A stringent gene annotation of *M. sibericum* was performed as previously described (13) using
414 RNA-seq transcriptomic data (6). Stranded RNA-seq reads were used to accurately annotate
415 protein-coding genes. Stringent gene annotation of *M. kamchatka* was performed w/o RNA seq
416 data but taking into account protein similarity with *M. sibericum*. Gene predictions were manually
417 curated using the web-based genomic annotation editing platform Web Apollo (25). Functional
418 annotations of protein-coding genes of both genomes were performed using a two-sided approach
419 as already previously described (13). Briefly, protein domains were searched with the CD-search
420 tool (26) and protein sequence searching based on the pairwise alignment of hidden Markov
421 models (HMM) was performed against the Uniclust30 database using HHblits tool (27). Gene
422 clustering was done using Orthofinder's default parameters (28) adding the "-M msa -oa" option.
423 Strict orthology between pairs of proteins was confirmed using best reciprocal blastp matches.

424 **Selection Pressure Analysis**

425 Ratios of non-synonymous (dN) over synonymous (dS) mutation rates for pairs of orthologous
426 genes were computed from MAFFT global alignment (29) using the PAML package and codeml with
427 the « model = 2 » (30). A strict filter was applyied to the dN/dS ratio: dN > 0, dS > 0, dS ≤ 2 and
428 dN/dS ≤ 10. The computation of the Codon Adaptation Index (CAI) of both Mollivirus was
429 performed using the cai tool from the Emboss package (31).

430 **Metagenome sequencing, assembly and annotation**

431 All metagenomic sample were sequenced with DNA-seq paired-end protocol on Illumina HiSeq
432 platform at Genoscope producing 16 datasets of 2x150bp read length. Raw reads quality was
433 evaluated with FASTQC (32). Identified contaminants were removed and remaining reads were
434 trimmed on the right end using 30 as quality threshold with BBTools (33). Assemblies of filtered
435 data sets were performed using MEGAHIT (34) with the following options: "--k-list 33,55,77,99,127
436 --min-contig-len 1000". All filtered reads were then mapped to the generated contigs using
437 Bowtie2 (35) with the "--very-sensitive" option.

438 **Availability of data**

439 The *M. kamtchatka* annotated genome sequence is freely available from the public through the
440 Genbank repository (URL://www.ncbi.nlm.nih.gov/genbank/) under accession number XXXXX.

441

442 **Acknowledgements**

443 We are deeply indebted to our volunteer collaborator Alexander Morawitz for collecting the
444 Kamchatka soil sample. We thank N. Brouilly, F. Richard and A. Aouane (imagery platform, Institut
445 de Biologie du Développement de Marseille Luminy) for their expert assistance. E Christo-Foroux is
446 the recipient of a DGA-MRIS scholarship (201760003). This project has received funding from the
447 European Research Council (ERC) under the European Union's Horizon 2020 research and
448 innovation program (grant agreement No 832601) and from the FRM prize "Lucien Tartois" to C.

Abergel. The funding bodies had no role in the design of the study, analysis, and interpretation of data and in writing the manuscript.

Competing interests

The authors declare that they have no competing interests

454 **Figures**

455

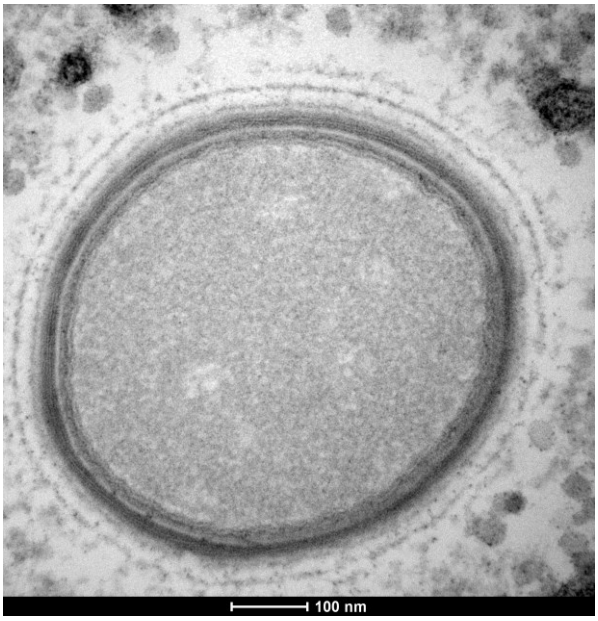

456

457 **Fig 1.** Ultrathin section TEM image of a neo-synthetized *M. kamchatka* particle in the cell

458 cytoplasm 7h post infection. The structure of the mature particles appear identical to that of *M.*

459 *sibericum.*

460

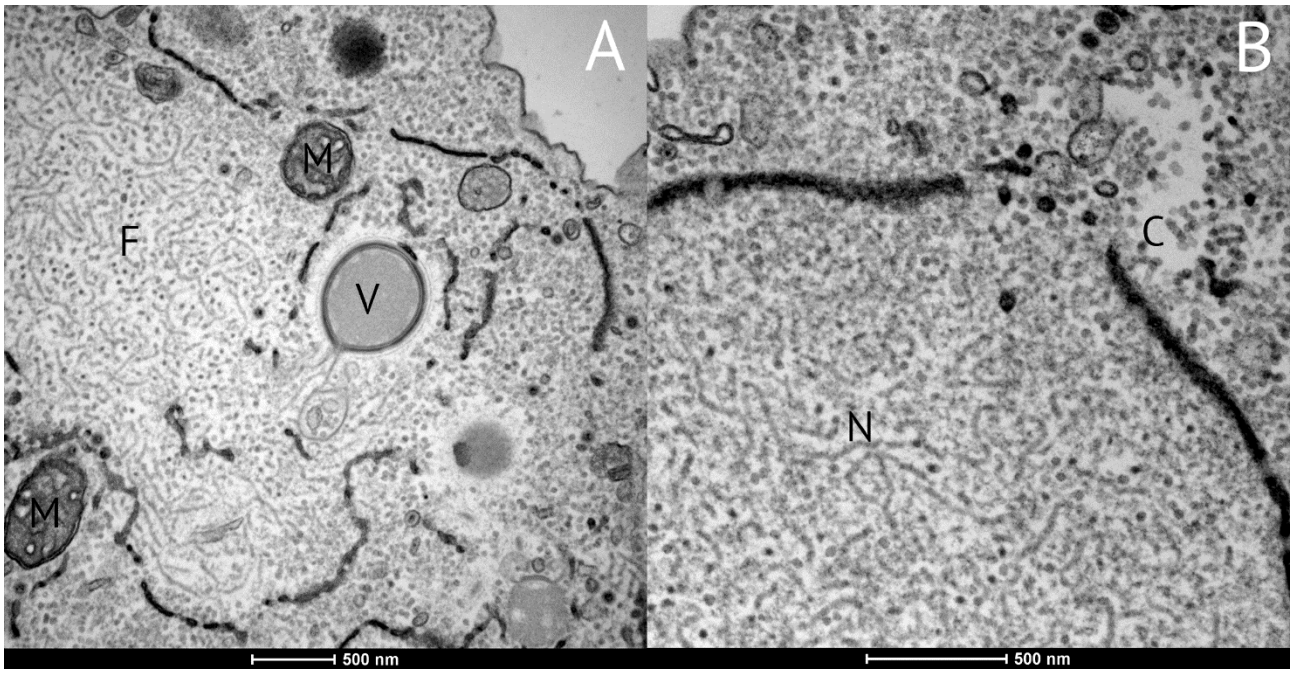

Fig 2. Ultrathin section TEM image of *A. castellanii* cell 7 to 10 hours post infection by *M. kamchatka***.** (A) Viral factory exhibiting fibrils (F), a nascent viral particle (V), and surrounding mitochondria (M). Fragments of the ruptured nuclear membrane are visible as dark bead strings. (B) Details of a nuclear membrane rupture through which fibrils synthetized in the nucleus (N) are shed into the cytoplasm (C).

469

470

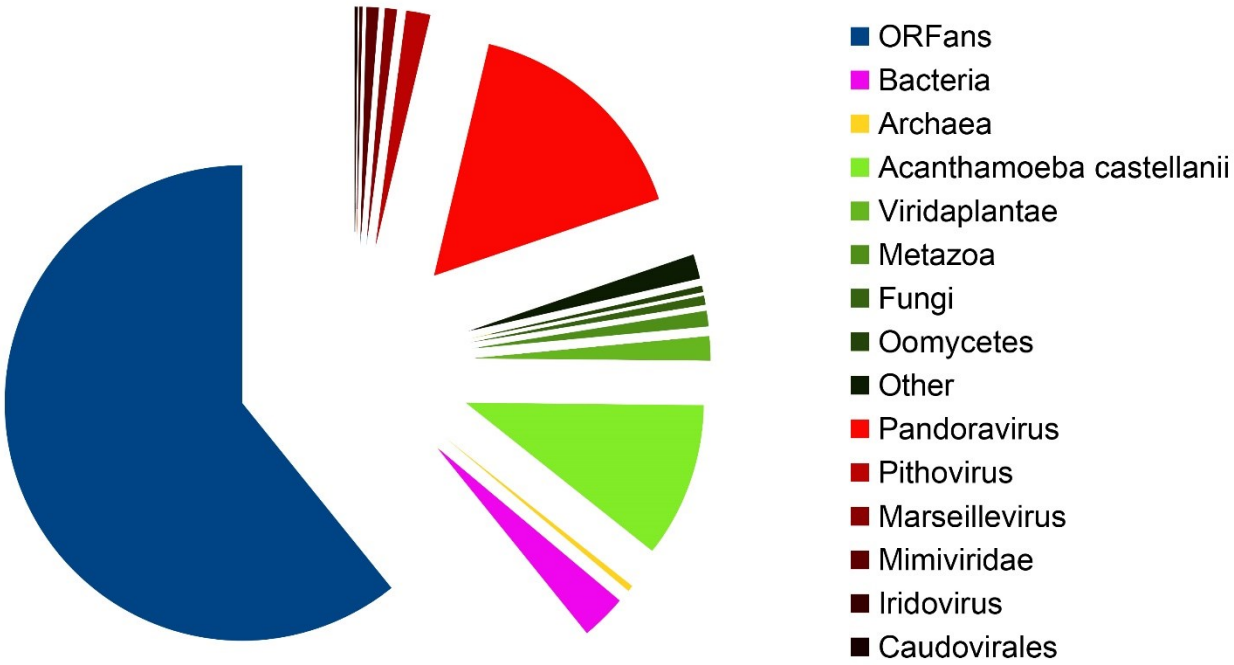

471

472 **Fig 3.** Distribution of the best-matching NR homologs of *M. kamchatka* predicted proteins. Best-
473 matching homologous proteins were identified using BLASTP (E value $<10^{-5}$) against the non-
474 redundant (NR) database (15) (after excluding *M. sibericum*). Green shades are used for
475 eukaryotes, red shades for viruses.

476

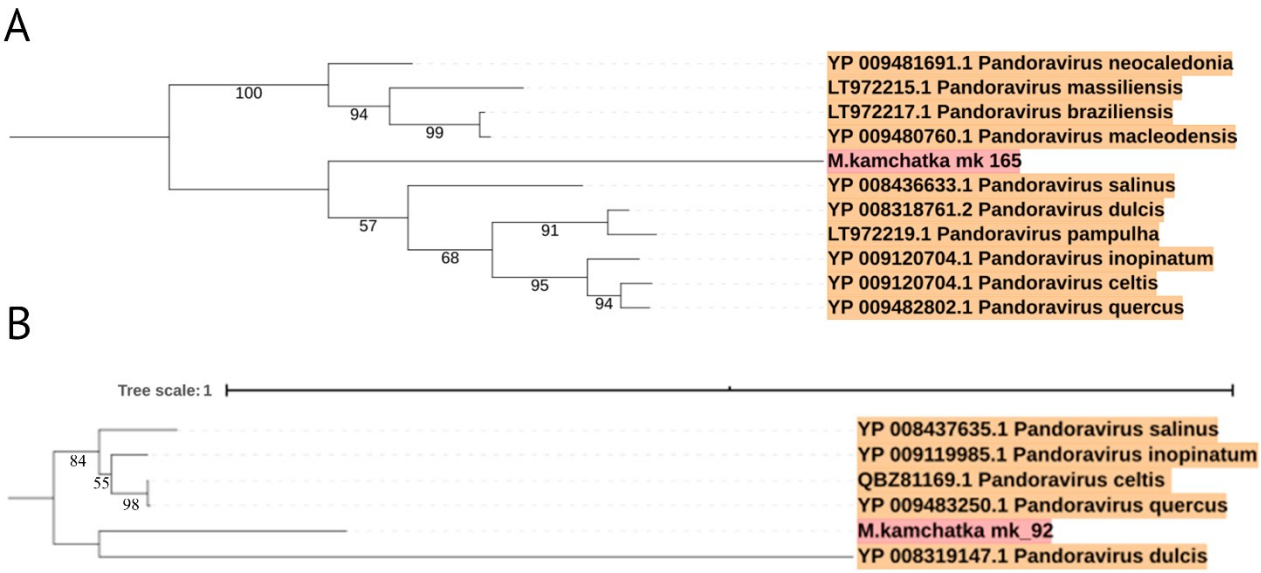

Fig 4. Eventual gene transfers from a pandoravirus to *M. kamchatka*. Both phylogenetic trees were computed from the global alignments of orthologous protein sequences using MAFFT (29). IQtree (36) was used to determine the optimal substitution model (options: « -m TEST » and « –bb 1000 »). (A) Protein mk_165 (no predicted function). (B) Predicted methyltransferase mk_92. Both *M. kamchatka* protein sequences appear embedded within the pandoravirus trees. In (A), the long branch leading to the *M. kamchatka* homolog suggests its accelerated divergence after an ancient acquisition from a pandoravirus. In (B), the long branch leading to the *P. dulcis* homolog might alternatively be interpreted as a non-orthologous replacement of the ancestral pandoravirus version of the gene.

489

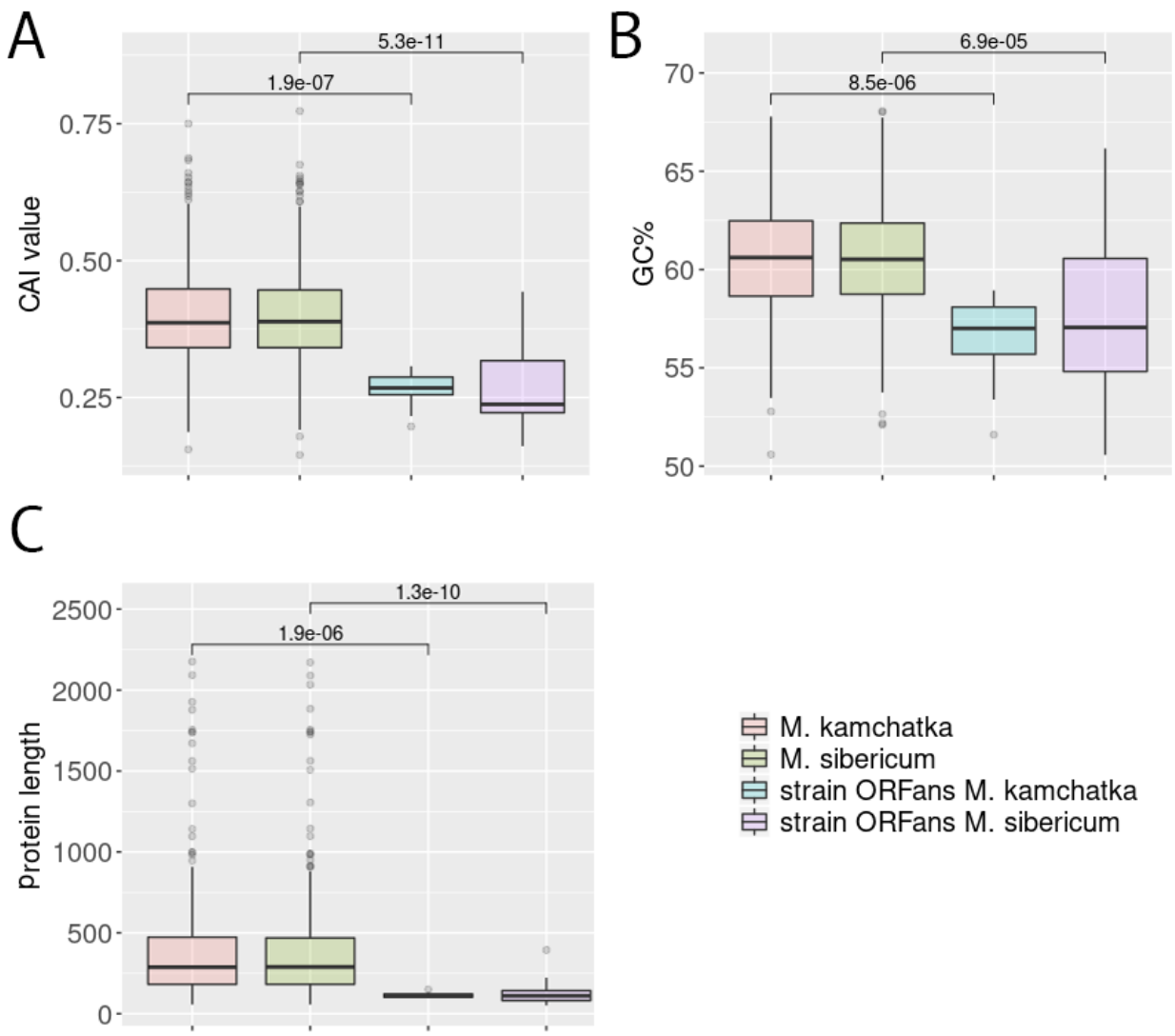

490

491

492 **Fig 5.** Genomic features of strain-specific ORFans. (A) Codon adaption index (CAI). (B) G+C content.

493 (C) Protein length. Box plots show the median, the 25th and 75th percentiles. P-value are

494 calculated using the Wilcoxon test.

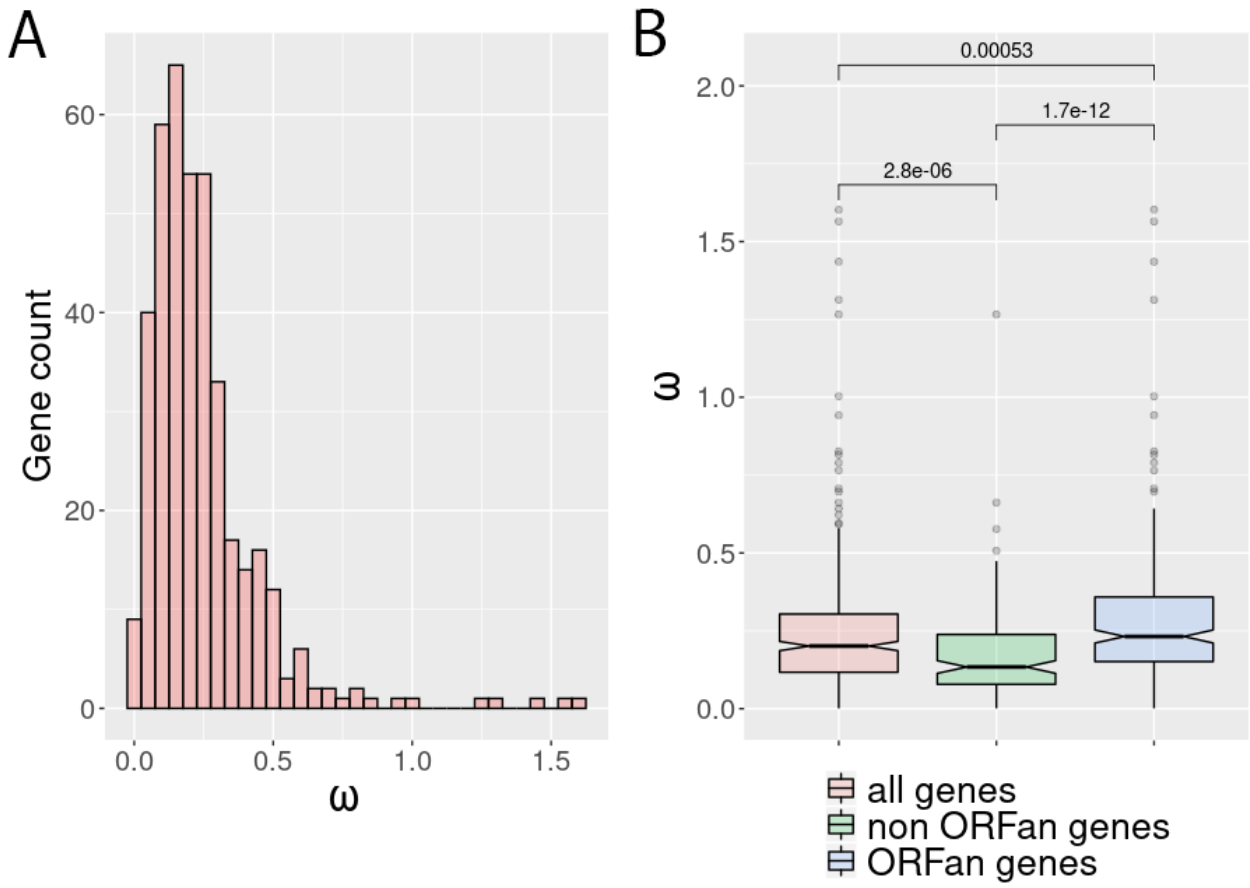

Fig 6. Selection pressure among different classes of genes. Values of ω (i.e. dN/dS) were computed from the alignments of homologous coding regions in *M. kamchatka* and *M. sibericum*. (A) Distribution of calculated ω values (n=397). (B) Box plots of the ω ratio among ORFan genes (n=243) and non ORFan genes (n=154). Box plots show the median, the 25th, and 75th percentiles. All p-value are calculated using the Wilcoxon test.

503

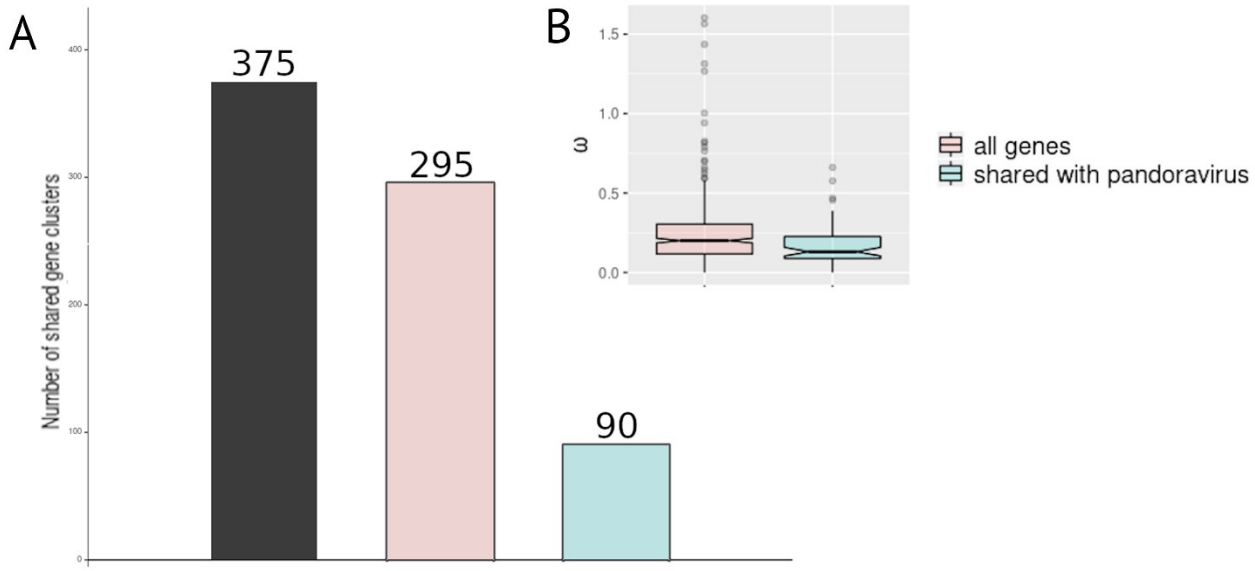

504

505 **Fig 7.** Comparison of the mollivirus and pandoravirus core gene contents. (A) The distribution of

506 the protein clusters shared by all pandoraviruses (black), the two Molliviruses (pink), and by both

507 virus groups (super core genes) (blue). (B) Box plot of ω values calculated from the alignment of

508 molliviruses core genes (pink), and super core genes (blue). Box plots show the median, the 25th,

509 and 75th percentiles.

510

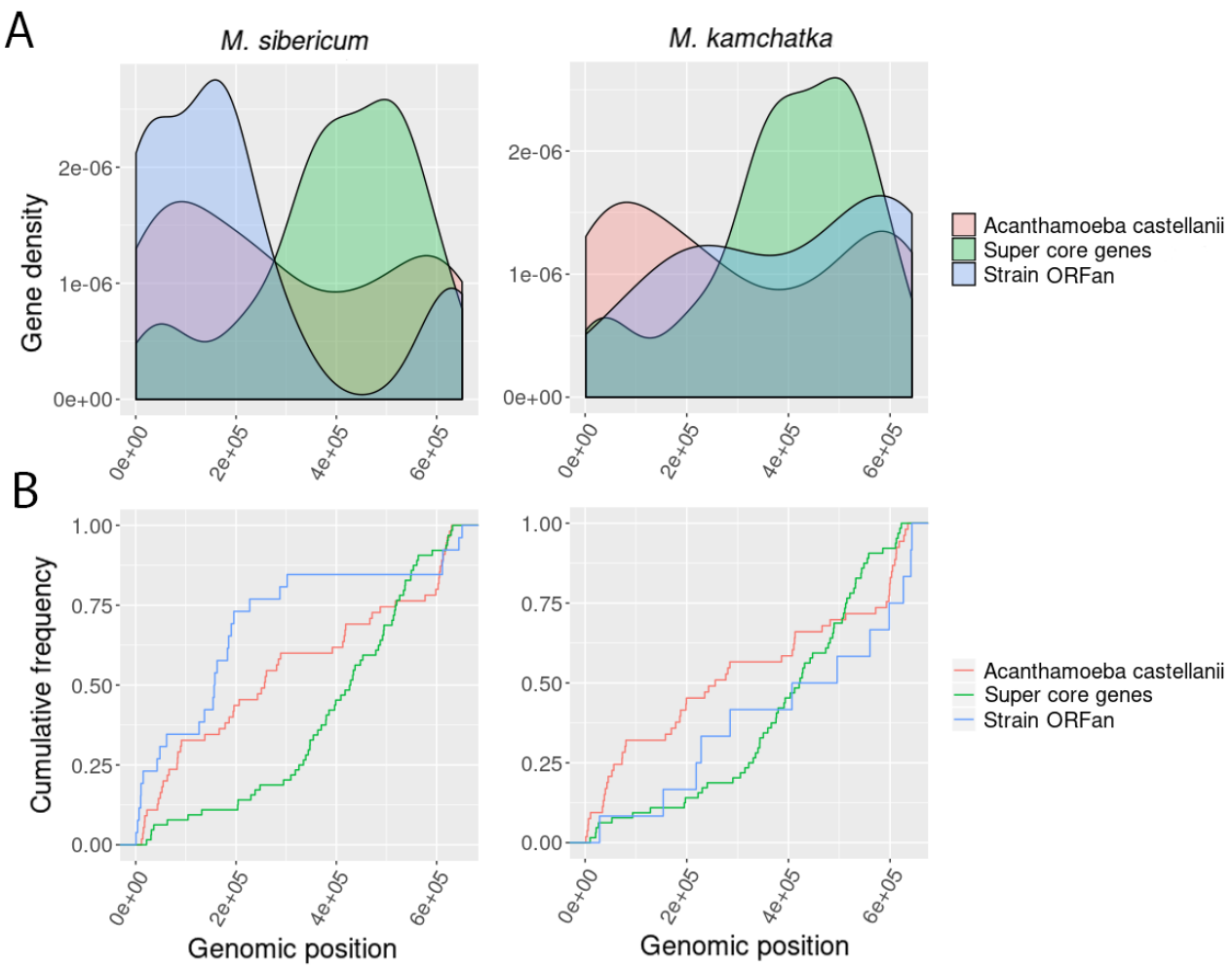

511

512 **Fig 8.** Distribution of different classes of genes along mollivirus genomes. (A) Variation of the gene

513 density as computed by the ggplot2 "geom_density" function (37). Genes with best-matching

514 homologs in *A. castellanii* (in the NR database excluding mollivirus) are uniformly distributed (in

515 pink) in contrast to super core genes (in green) and strain-specific ORFans (in blue). (B) Cumulative

516 distribution of the above classes of genes using the same color code.

517

518

519

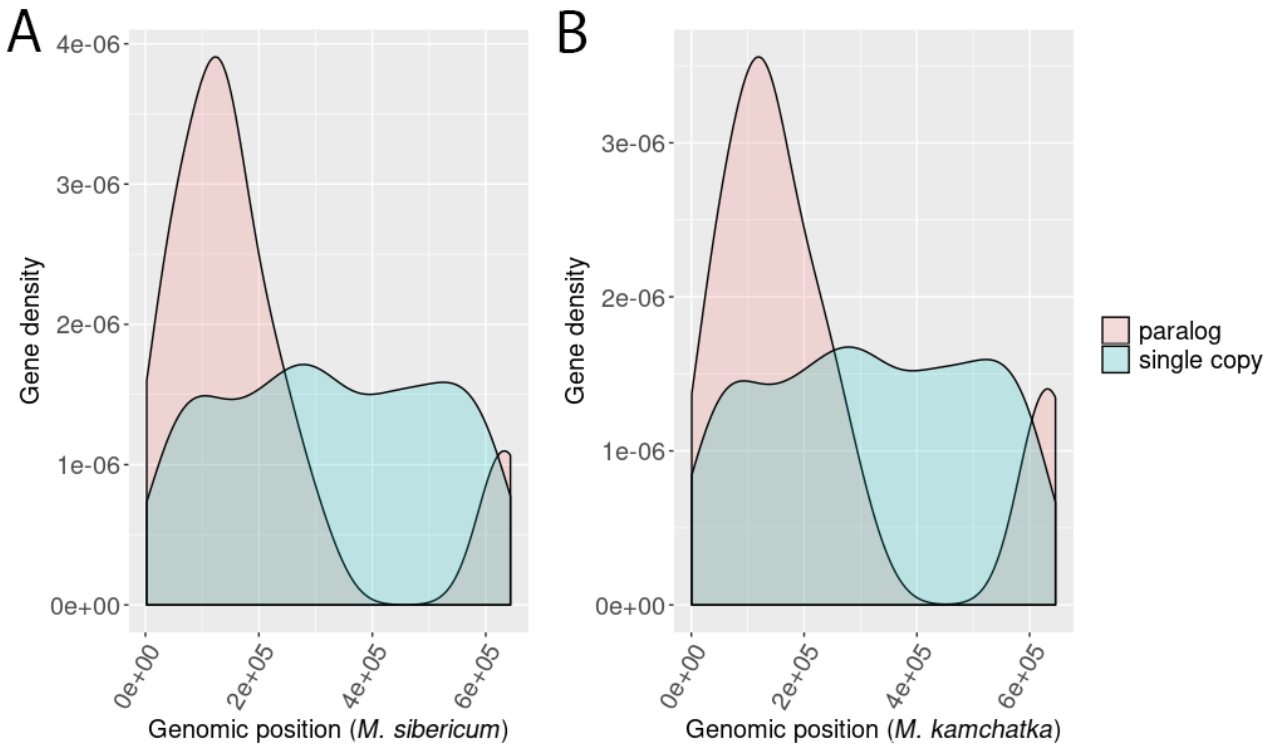

520

521 **Fig 9.** Distribution of single-copy *vs.* multiple copy genes along mollivirus genomes. Single copy

522 genes (in blue) in both strains are uniformly distributed in contrast to genes with paralogs (pink) in

523 at least one strain that cluster in the left half of the genomes. (A) *M. sibericum* (n=48). (B) *M.*

524 *kamchatka* (n= 46).

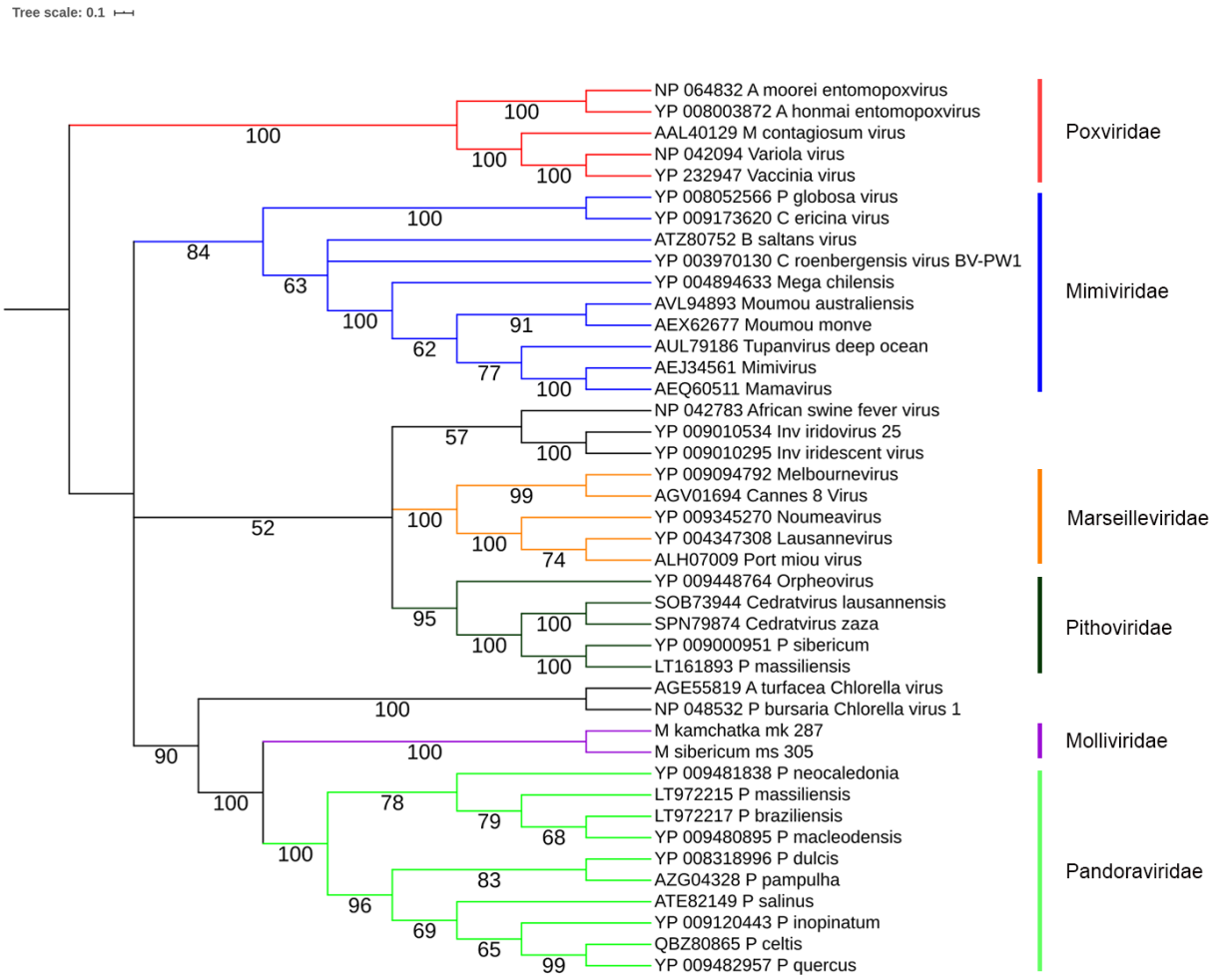

Fig 10. Phylogeny of DNA polymerase B of large and giant dsDNA viruses. This neighbor-joining tree was computed (JTT substitution model, 100 resampling) on 397 amino acid positions from an alignment of 42 sequences computed by MAFFT (29). Branches with boostrap values <60% were collapsed.

531 **Tables**

532

533 **Table 1.** Status of the protein-coding genes unique to *M. kamchatka*

ORF ID	Predicted function	Putative evolutionary scenario
mk_25	None (ORFan)	*de novo* creation or loss in *M. sibericum*
mk_92	DNA methyltransferase	loss in *M. sibericum* (present in some pandoraviruses)
mk_93	Ring domain	loss in *M. sibericum* (present in some pandoraviruses)
mk_104	Ring domain	loss in *M. sibericum* (present in some pandoraviruses)
mk_127	None (ORFan)	*de novo* creation or loss in *M. sibericum*
mk_159	None	loss in *M. sibericum* (present in some pandoraviruses)
mk_165	None	HGT from Pandoravirus
mk_166	Peptidase	loss in *M. sibericum* (present in some pandoraviruses)
mk_172	None (ORFan)	*de novo* creation or loss in *M. sibericum*
mk_182	None (ORFan)	*de novo* creation or loss in *M. sibericum*
mk_231	None (ORFan)	*de novo* creation or loss in *M. sibericum*
mk_313	None (ORFan)	*de novo* creation or loss in *M. sibericum*
mk_369	None (ORFan)	*de novo* creation or loss in *M. sibericum*
mk_415	None (ORFan)	*de novo* creation or loss in *M. sibericum*
mk_441	None (ORFan)	*de novo* creation or loss in *M. sibericum*
mk_466	None (ORFan)	*de novo* creation or loss in *M. sibericum*
mk_467	None	loss in *M. sibericum* (HGT to Acanthamoeba)
mk_469	B1-1 like	loss in *M. sibericum* (present in Acanthamoeba)
mk_476	None (ORFan)	*de novo* creation or loss in *M. sibericum*
mk_478	None (ORFan)	*de novo* creation or loss in *M. sibericum*

534

535 **Table 2.** Status of the protein-coding genes unique to *M. sibericum*

ORF ID	Predicted function	**Putative evolutionary scenario**
ms_1	None (ORFan)	*De novo* creation or loss in *M. kamchatka*
ms_3	None (ORFan)	*De novo* creation or loss in *M. kamchatka*
ms_5	None (ORFan)	*De novo* creation or loss in *M. kamchatka*
ms_7	None (ORFan)	*De novo* creation or loss in *M. kamchatka*
ms_8	None (ORFan)	*De novo* creation or loss in *M. kamchatka*
ms_13	None (ORFan)	*De novo* creation or loss in *M. kamchatka*
ms_14	None	HGT to Acanthamoeba
ms_38	None (ORFan)	*De novo* creation or loss in *M. kamchatka*
ms_42	None (ORFan)	*De novo* creation or loss in *M. kamchatka*
ms_53	None (ORFan)	*De novo* creation or loss in *M. kamchatka*
ms_64	None	loss in *M. Kamchatka* (present in Noumeavirus)
ms_109	None (ORFan)	*De novo* creation or loss in *M. kamchatka*
ms_120	None (ORFan)	*De novo* creation or loss in *M. kamchatka*
ms_136	None (ORFan)	*De novo* creation or loss in *M. kamchatka*
ms_138	None (ORFan)	*De novo* creation or loss in *M. kamchatka*
ms_139	None (ORFan)	*De novo* creation or loss in *M. kamchatka*
ms_144	None (ORFan)	*De novo* creation or loss in *M. kamchatka*
ms_157	None (ORFan)	*De novo* creation or loss in *M. kamchatka*
ms_159	None (ORFan)	*De novo* creation or loss in *M. kamchatka*
ms_166	None (ORFan)	*De novo* creation or loss in *M. kamchatka*
ms_172	None (ORFan)	*De novo* creation or loss in *M. kamchatka*
ms_190	None	loss in *M. kamchatka* (present in some pandoraviruses)
ms_193	None (ORFan)	*De novo* creation or loss in *M. kamchatka*
ms_246	None (ORFan)	*De novo* creation or loss in *M. kamchatka*
ms_258	None (ORFan)	*De novo* creation or loss in *M. kamchatka*
ms_311	Zinc-finger domain	loss in *M. kamchatka (*present in *Gossypium hirsutum)*
ms_312	Zinc-finger domain	loss in *M. kamchatka* (present in *Cavenderia fasciculata)*
ms_313	None	loss in *M. kamchatka* (present in some pandoraviruses)
ms_464	None (ORFan)	*De novo* creation or loss in *M. kamchatka*
ms_465	None (ORFan)	*De novo* creation or loss in *M. kamchatka*
ms_479	DNA methyltransferase	loss in *M. kamchatka* (present in some pandoraviruses)
ms_494	None (ORFan)	*De novo* creation or loss in *M. kamchatka*
ms_495	None (ORFan)	*De novo* creation or loss in *M. kamchatka*

536

537

538 **References**

539 1. Shi T, Reeves RH, Gilichinsky DA, Friedmann EI, 1997. Characterization of Viable Bacteria from
540 Siberian Permafrost by 16S rDNA Sequencing. Microb Ecol 33:169-179.
541 https://doi.org/10.1007/s002489900019.
542 2. Vishnivetskaya T, Kathariou S, McGrath J, Gilichinsky D, Tiedje JM 2000. Low-temperature
543 recovery strategies for the isolation of bacteria from ancient permafrost sediments. Extremophiles
544 4:165-173. https://doi.org/10.1007/s007920070031.
545 3. Graham DE, Wallenstein MD, Vishnivetskaya TA, Waldrop MP, Phelps TJ, Pfiffner SM, Onstott TC,
546 Whyte LG, Rivkina EM, Gilichinsky DA, Elias DA, Mackelprang R, VerBerkmoes NC, Hettich RL,
547 Wagner D, Wullschleger SD, Jansson JK. 2012. Microbes in thawing permafrost: the unknown
548 variable in the climate change equation. ISME J 6:709-712.
549 https://doi.org/10.1038/ismej.2011.163.
550 4. Yashina S, Gubin S, Maksimovich S, Yashina A, Gakhova E, Gilichinsky D. 2012. Regeneration of
551 whole fertile plants from 30,000-y-old fruit tissue buried in Siberian permafrost. Proc Natl Acad Sci
552 U S A 109:4008-4013. https://doi.org/10.1073/pnas.1118386109.
553 5. Legendre M, Bartoli J, Shmakova L, Jeudy S, Labadie K, Adrait A, Lescot M, Poirot O, Bertaux L,
554 Bruley C, Couté Y, Rivkina E, Abergel C, Claverie JM. 2014. Thirty-thousand-year-old distant relative
555 of giant icosahedral DNA viruses with a pandoravirus morphology. Proc Natl Acad Sci U S A
556 111:4274-4279. https://doi.org/ 10.1073/pnas.1320670111.
557 6. Legendre M, Lartigue A, Bertaux L, Jeudy S, Bartoli J, Lescot, M, Alempic JM, Ramus C, Bruley C,
558 Labadie K, Shmakova L, Rivkina E, Couté Y, Abergel C, Claverie JM. 2015. In-depth study of
559 Mollivirus sibericum, a new 30,000-y-old giant virus infecting Acanthamoeba. Proc Natl Acad Sci U
560 S A 112:E5327-E5335. https://doi.org/10.1073/pnas.1510795112.

561 7. Abergel C, Legendre M, Claverie JM. The rapidly expanding universe of giant viruses: Mimivirus,
562 Pandoravirus, Pithovirus and Mollivirus. 2015. FEMS Microbiol Rev 39:779-796.
563 https://doi.org/10.1093/femsre/fuv037.
564 8. Levasseur A, Andreani J, Delerce J, Bou Khalil J, Robert C, La Scola B, Raoult D. 2016. Comparison
565 of a Modern and Fossil Pithovirus Reveals Its Genetic Conservation and Evolution. Genome Biol
566 Evol 8:2333-2339. https://doi.org/10.1093/gbe/evw153.
567 9. Andreani J, Aherfi S, Bou Khalil JY, Di Pinto F, Bitam I, Raoult D, Colson P, La Scola B. 2016.
568 Cedratvirus, a Double-Cork Structured Giant Virus, is a Distant Relative of Pithoviruses. Viruses
569 8:300. https://doi.org/10.3390/v8110300.
570 10. Bertelli C, Mueller L, Thomas V, Pillonel T, Jacquier N, Greub G. 2017. Cedratvirus lausannensis -
571 digging into Pithoviridae diversity. Environ Microbiol 19:4022-4034.
572 https://doi.org/10.1111/1462-2920.13813.
573 11. Quemin ER, Corroyer-Dulmont S, Baskaran A, Penard E, Gazi AD, Christo-Foroux E, Walther P,
574 Abergel C, Krijnse-Locker J. 2019. Complex membrane remodeling during virion assembly of the
575 30,000-year-old Mollivirus sibericum. J Virol 93(13). pii: e00388-19.
576 https://doi.org/10.1128/JVI.00388-19.
577 12. Philippe N, Legendre M, Doutre G, Couté Y, Poirot O, Lescot M, Arslan D, Seltzer V, Bertaux L,
578 Bruley C, Garin J, Claverie JM, Abergel C. 2013. Pandoraviruses: amoeba viruses with genomes up
579 to 2.5 Mb reaching that of parasitic eukaryotes. Science 341:281-286.
580 https://doi.org/10.1126/science.1239181.
581 13. Legendre M, Fabre E, Poirot O, Jeudy S, Lartigue A, Alempic JM, Beucher L, Philippe N, Bertaux
582 L, Christo-Foroux E, Labadie K, Couté Y, Abergel C, Claverie JM. 2018. Diversity and evolution of the
583 emerging Pandoraviridae family. Nat Commun 9:2285.
584 https://doi.org/10.1038/s41467-018-04698-4.

585 14. Legendre M, Alempic JM, Philippe N, Lartigue A, Jeudy S, Poirot O, Ta NT, Nin S, Couté Y,
586 Abergel C, Claverie JM. 2019. Pandoravirus celtis illustrates the microevolution processes at work
587 in the giant Pandoraviridae genomes. Front Microbiol 10:430. https://doi.org/
588 10.3389/fmicb.2019.00430.
589 15. NCBI Resource Coordinators. 2018. Database resources of the National Center for
590 Biotechnology Information. Nucleic Acids Res 46:D8-D13. https://doi.org/10.1093/nar/gkx1095.
591 16. Heidel AJ, Lawal HM, Felder M, Schilde C, Helps NR, Tunggal B, Rivero F, John U, Schleicher M,
592 Eichinger L, Platzer M, Noegel AA, Schaap P, Glöckner G. 2011. Phylogeny-wide analysis of social
593 amoeba genomes highlights ancient origins for complex intercellular communication. Genome Res
594 21:1882-1891. https://doi.org/10.1101/gr.121137.111.
595 17. Thomas V, Bertelli C, Collyn F, Casson N, Telenti A, Goesmann A, Croxatto A, Greub G. 2011.
596 Lausannevirus, a giant amoebal virus encoding histone doublets. Environ Microbiol 13:1454-1466.
597 https://doi.org/10.1111/j.1462-2920.2011.02446.x.
598 18. Maumus F, Blanc G. 2016. Study of gene trafficking between acanthamoeba and giant viruses
599 suggests an undiscovered fof amoeba-infecting viruses. Genome Biol
600 Evol 8:3351-3363. https://doi.org/10.1093/gbe/evw260.
601 19. Chelkha N, Levasseur A, Pontarotti P, Raoult D, Scola B, Colson P. 2018. A phylogenomic study of
602 *Acanthamoeba polyphaga* draft genome sequences suggests genetic exchanges with giant viruses.
603 Front Microbiol 9:2098. https://doi.org/10.3389/fmicb.2018.02098.
604 20. Duchêne S, Holmes EC. 2018. Estimating evolutionary rates in giant viruses using
605 ancient genomes. Virus Evol 4:vey006. https://doi.org/10.1093/ve/vey006.
606 21. Hughes AL, Irausquin S, Friedman R. 2010. The evolutionary biology of poxviruses. Infect Genet
607 Evol 10:50-59. https://doi.org/10.1016/j.meegid.2009.10.001.
608 22. San Martín C, van Raaij MJ. 2018. The so far farthest reaches of the double jelly roll capsid
609 protein fold. Virol J 15:181. https://doi.org/10.1186/s12985-018-1097-1.

610 23. Arslan D, Legendre M, Seltzer V, Abergel C, Claverie JM. 2011. Distant Mimivirus relative with a
611 larger genome highlights the fundamental features of Megaviridae. Proc Natl Acad Sci U S A
612 108:17486-17491. https://doi.org/10.1073/pnas.1110889108.
613 24. Bankevich A, Nurk S, Antipov D, Gurevich A, Dvorkin M, Kulikov AS, Lesin V, Nikolenko S, Pham
614 S, Prjibelski A, Pyshkin A, Sirotkin A, Vyahhi N, Tesler G, Alekseyev MA, Pevzner P. 2012. SPAdes: A
615 New Genome Assembly Algorithm and Its Applications to Single-Cell Sequencing. J Comput Biol
616 19:455-477. https://doi.org/10.1089/cmb.2012.0021.
617 25. Dunn NA, Unni DR, Diesh C, Munoz-Torres M, Harris NL, Yao E, Rasche H, Holmes I, Elsik C,
618 Lewis S. 2019. Apollo: Democratizing genome annotation. PLoS Comput Biol 15: e1006790.
619 https://doi.org/10.1371/journal.pcbi.1006790.
620 26. Marchler-Bauer A, Derbyshire MK, Gonzales NR, Lu S, Chitsaz F, Geer LY, Geer RC, He J, Gwadz
621 M, Hurwitz DI, Lanczycki CJ, Lu F, Marchler GH, Song JS, Thanki N, Wang Z, Yamashita RA, Zhang D,
622 Zheng C, Bryant SH. 2015. CDD: NCBI's conserved domain database. Nucleic Acids Res 43:D222-
623 226. https://doi.org/10.1093/nar/gku1221.
624 27. Remmert M, Biegert A, Hauser A, Söding J. 2011. HHblits: lightning-fast iterative
625 protein sequence searching by HMM-HMM alignment. Nat Methods. 9:173-175.
626 https://doi.org/10.1038/nmeth.1818.
627 28. Emms DM, Kelly S. 2015. OrthoFinder: solving fundamental biases in whole genome
628 comparisons dramatically improves orthogroup inference accuracy. Genome Biol 16:157.
629 https://doi.org/10.1186/s13059-015-0721-2.
630 29. Katoh K, Misawa K, Kuma K-I, Miyata T. 2002. MAFFT: a novel method for rapid multiple
631 sequence alignment based on fast Fourier transform. Nucleic Acids Res 30:3059-3066.
632 https://doi.org/10.1093/nar/gkf436.
633 30. Yang Z. 2007. PAML 4: phylogenetic analysis by maximum likelihood. Mol Biol Evol 24:1586-
634 1591. https://doi.org/10.1093/molbev/msm088.

635 31 . Rice P, Longden I, Bleasby A. 2000. EMBOSS: the European molecular biology open software
636 suite. Trends Genet 16:276-277. https://doi.org/10.1016/s0168-9525(00)02024-2.
637 32. Andrews S. 2010. FastQC: a quality control tool for high throughput sequence data. Available
638 online at: http://www.bioinformatics.babraham.ac.uk/projects/fastqc .
639 33. Bushnell B, Rood J, Singer E. 2017. BBMerge – Accurate paired shotgun read merging via
640 overlap. PLoS ONE 12: e0185056. https://doi.org/10.1371/journal.pone.0185056.
641 34. Li D, Liu C-M, Luo R, Sadakane K, Lam T-W. 2015. MEGAHIT: An ultra-fast single-node solution
642 for large and complex metagenomics assembly via succinct de Bruijn graph. Bioinformatics
643 31:1674-1676. https://doi.org/10.1093/bioinformatics/btv033.
644 35. Langmead B, Salzberg SL. 2012. Fast gapped-read alignment with Bowtie 2. Nat Methods
645 9:357-359. https://doi.org/10.1038/nmeth.1923.
646 36. Nguyen LT, Schmidt HA, von Haeseler A, Minh BQ. 2015. IQ-TREE: A fast and effective stochastic
647 algorithm for estimating maximum likelihood phylogenies. Mol Biol Evol 32:268-274.
648 https://doi.org/10.1093/molbev/msu300.
649 37. Wickham H. ggplot2: Elegant Graphics for Data Analysis, p 33-74. 2016. Springer-Verlag New
650 York.